

# 真空紫外光电离质谱法在烟气老化研究中的应用

马 兰<sup>1,2</sup>, 温作赢<sup>1</sup>, 彭晓萌<sup>3</sup>, 赵 锋<sup>1,2</sup>, 叶绍鑫<sup>1,2</sup>,  
谢 恺<sup>1,2</sup>, 顾学军<sup>1</sup>, 王 健<sup>3</sup>

(1. 中国科学院合肥物质科学研究院安徽光学精密机械研究所, 安徽 合肥 230031; 2. 中国科学技术大学, 安徽 合肥 230026;  
3. 安徽中烟工业有限责任公司, 烟草化学安徽省重点实验室, 安徽 合肥 230088)

**摘要:** 本文应用自主研发的真空紫外光电离飞行时间质谱仪, 原位在线检测燃烧型卷烟、加热不燃烧型卷烟和电子烟产生的烟气气溶胶, 表征其气相成分及颗粒相成分。结果表明, 3 种烟气气溶胶的化学组成差异显著, 其中燃烧型卷烟的成分含量及物种丰度远大于新型烟草制品, 其气相和颗粒相的整体信号强度分别约为新型烟草制品的 100 倍和 10 倍。检出的气溶胶成分中含有大量不饱和化合物, 这些物质在环境中极易被氧化并生成新的超细颗粒物。结合 Teflon 反应腔分别模拟以上 3 种类型的烟气气溶胶在不同臭氧浓度下的老化过程, 结果均有超细颗粒物生成。超细颗粒物的形成条件与前体物的含量和成分分布有关, 燃烧型卷烟气溶胶在室内 O<sub>3</sub> 浓度下就可以很快形成超细颗粒物, 而新型烟草制品则需要更高浓度的 O<sub>3</sub> 或更长的老化时间。

**关键词:** 光电离质谱; 在线测量; 烟气老化; 超细颗粒物; 室内污染

中图分类号: O657.63 文献标志码: A 文章编号: 1004-2997(2024)05-0656-10

doi: [10.7538/zpxb.2024.0023](https://doi.org/10.7538/zpxb.2024.0023)

## Application of Vacuum Ultraviolet Photoionization Mass Spectrometry in the Aging Study of Smoke Aerosols

MA Lan<sup>1,2</sup>, WEN Zuo-ying<sup>1</sup>, PENG Xiao-meng<sup>3</sup>, ZHAO Feng<sup>1,2</sup>, YE Shao-xin<sup>1,2</sup>,  
XIE Kai<sup>1,2</sup>, GU Xue-jun<sup>1</sup>, WANG Jian<sup>3</sup>

(1. Anhui Institute of Optics & Fine Mechanics, Hefei Institutes of Physical Science, Chinese Academy of Sciences,  
Hefei 230031, China; 2. University of Science and Technology of China, Hefei 230026, China; 3. Key Laboratory of  
Combustion and Pyrolysis, China Tobacco Anhui Industrial Co, Ltd, Hefei 230088, China)

**Abstract:** Smoke aerosols contain many harmful substances and have become one of the major sources of indoor pollutants. The smoke aerosols released into the environment are easy to react with various oxidants presented in the room, namely the aging process of the smoke aerosol, which can produce secondary organic aerosols. The chemical composition of smoke aerosol is an important factor affecting its indoor aging process, but so far, the change behavior of the composition and particle size distribution of smoke aerosol during the aging process remains to be studied, and the aging analysis of novel tobacco products has not been reported. Therefore, the present study applied a house-made vacuum ultraviolet photoionization time-of-flight mass spectrometer to detect the chemical composition of the smoke aerosols produced by combustion cigarette, and new tobacco

products, e.g., heat-not-burn tobacco products and e-cigarette, achieving the *in-situ* online characterization of their gas-phase and particulate-phase components. The results showed that the chemical composition of the smoke aerosols generated by the three types of tobacco products is significantly different, among which the component content and species abundance of the combustion cigarette are much greater than those of the novel tobacco products, and the overall signal intensity of combustion cigarette in the gas-phase and the particulate-phase is about 100 times and 10 times that of novel tobacco products, respectively. In addition, it was found that the particulate-phase mass spectra of novel tobacco products contain a large amount of glycerol, which is almost absent in combustion cigarette, and its intensity is even more than nicotine. The detected aerosol components contain many unsaturated compounds, which are easily oxidized in the environment and generate new ultrafine particles (UFPs). The Teflon chamber was used to simulate the aging process of the above three smoke aerosols with different O<sub>3</sub> concentrations. The results of scanning mobility particle sizer showed that UFPs are generated in all of them. Corresponding to the results of photoionization mass spectrometry, the aging processes of the three smoke aerosols are completely different, in which the formation conditions of UFPs are related to the content and composition distribution of precursors. Specifically, the indoor concentration of O<sub>3</sub> (observed in this experiment was 40 μg/m<sup>3</sup>) can promote the formation of UFPs with a geometric mean diameter of about 26 nm in the combustion cigarette, while the UFPs formation of novel tobacco products requires a higher concentration of O<sub>3</sub> or a longer aging time. This is mainly facts that the whole composition concentration of the novel tobacco products is much lower than that of combustion cigarette, and the particulate-phase components contain a lot of glycerol. Due to the strong viscosity and encapsulation, glycerol may exist in the particulate-phase of the smoke aerosol in the form of coating other substances, such as nicotine, and further prevents the aging process of other substances, resulting in differences in particle size distribution. This study explains the reason of difference in UFPs formation of various smoke aerosols during the aging process and provides a basis for tobacco exposure risk assessment, which is expected to reveal the aging mechanism of smoke aerosols in the future.

**Key words:** photoionization mass spectrometry; on-line detection; aging smoke aerosol; ultrafine particle; indoor pollution

烟气气溶胶含有多种有毒有害成分<sup>[1]</sup>,对人体健康危害较大,是室内污染物的主要来源之一<sup>[2]</sup>。近年来,出现了一系列新型烟草制品,如加热不燃烧型卷烟和电子烟。相比于传统的燃烧型卷烟,新型烟草制品不需要经过高温燃烧便可传递尼古丁,且在设计上避免了侧流烟气的产生,有效减少了有害和潜在有害物质的形成量和暴露量<sup>[3-5]</sup>。但研究表明<sup>[6-9]</sup>,这些新型烟草制品在使用过程中仍会不断释放有毒物质,直接影响室内环境质量和人体健康。

释放到环境中的烟气气溶胶会与室内存在的各类氧化剂作用<sup>[10-12]</sup>,经历烟气的老化过程,形成二次有机气溶胶,并生成毒性更大的氧化产物<sup>[13-14]</sup>。有研究表明<sup>[13,15]</sup>,燃烧型卷烟气溶胶在

室内O<sub>3</sub>的诱导下可产生新的超细颗粒物(粒径小于100 nm)。烟气气溶胶的化学成分是影响其室内老化过程的重要因素,目前,关于烟气气溶胶的成分及粒径分布在其老化过程中的变化行为还有待研究,而对于新型烟草制品的老化分析还尚未见报道。采用多种分析手段对不同种类烟气气溶胶的化学成分进行准确检测与表征,并分析其与老化过程中粒径分布的关系,已成为烟草暴露风险评估的重要基础。

针对烟气气溶胶的成分检测,传统方法主要为基于色谱与质谱联用的离线检测技术,如气相色谱-质谱和液相色谱-质谱等<sup>[16-18]</sup>。这些方法通常需要经历样品的离线富集及预处理过程,检测条件(如时间、温度等)会影响烟气气溶胶的化

学成分在气相和颗粒相中的分布<sup>[19]</sup>,因此较难获得新鲜烟气气溶胶的化学成分信息。近些年,傅里叶变换红外光谱(FTIR)<sup>[20]</sup>、红外激光光谱<sup>[21]</sup>以及基于激光共振增强多光子电离(REMPI)或真空紫外灯单光子电离的光电离质谱(PIMS)<sup>[22-24]</sup>等方法被广泛应用于表征烟气气溶胶的气相成分。但由于烟气气溶胶中的颗粒相成分较复杂,能够直接对其进行原位检测的技术较少。Barsanti等<sup>[25]</sup>将核磁共振波谱(NMR)技术应用于卷烟颗粒物的原位化学分析,但获得的成分信息有限,且谱图分析复杂。其他检测方法,如基于激光电离的气溶胶飞行时间质谱<sup>[26]</sup>、实时直接分析质谱(DART-MS)<sup>[27]</sup>及化学电离质谱(CIMS)<sup>[28]</sup>等也被应用于烟气颗粒物的成分检测,但这些研究多关注于颗粒物收集、稀释及汽化等技术的创新,未能获得全面的成分信息。

基于此,本工作拟应用自主研发的真空紫外光电离飞行时间质谱(VUV-TOF MS)仪对传统的燃烧型卷烟以及加热不燃烧型卷烟和电子烟2种新型烟草制品的化学成分进行对比研究,通过吸烟机与光电离质谱仪的毛细管进样口或空气动力学透镜进样系统直接相连,实现各类烟气气溶胶气相成分和颗粒相成分的原位在线检测。同时,采用Teflon反应腔模拟3种烟气气溶胶在不同O<sub>3</sub>浓度下的室内老化过程,并利用扫描电迁移率粒径谱仪实时监测老化过程中的粒

径迁移及粒子数浓度,尤其关注老化过程中超细颗粒物的生成情况。最后,结合光电离质谱获得的成分信息对不同类型烟气气溶胶老化过程中的粒谱进行分析。

## 1 实验装置与方法

实验装置示于图1,主要包括吸烟机、150 L的Teflon反应腔、扫描电迁移率粒径谱(SMPS)仪和自主研制的VUV-TOF MS仪。

本实验使用的吸烟机为商品化单孔道直线型吸烟机,主要由烟嘴、电磁三通阀和柱塞组成。将样品的抽吸端塞入吸烟机的烟嘴处,由电脑端的程序软件自动控制吸烟机以模拟吸烟者的吸烟行为,并按照加拿大卫生部深度抽吸模式(HCI, 55 cm<sup>3</sup>/2 s)进行抽吸。

采用VUV-TOF MS分别对烟气气溶胶的气相成分和颗粒相成分进行原位在线检测,仪器检测原理可参考本课题组先前的研究<sup>[29]</sup>。所有样品均由吸烟机采集,随后直接通过光电离质谱的不同进样接口进入检测区。当检测气相成分时,需要在吸烟机的烟嘴处塞入剑桥滤片以去除气溶胶中的颗粒物,随后样品由光电离质谱仪的毛细管进样口进入检测区。毛细管内径0.1 mm,长度约4 cm,进样流量4 cm<sup>3</sup>/min,将其温度设为70 °C,以避免挥发性有机化合物(VOCs)在内部冷凝。当检测颗粒相成分时,样品直接由光电离

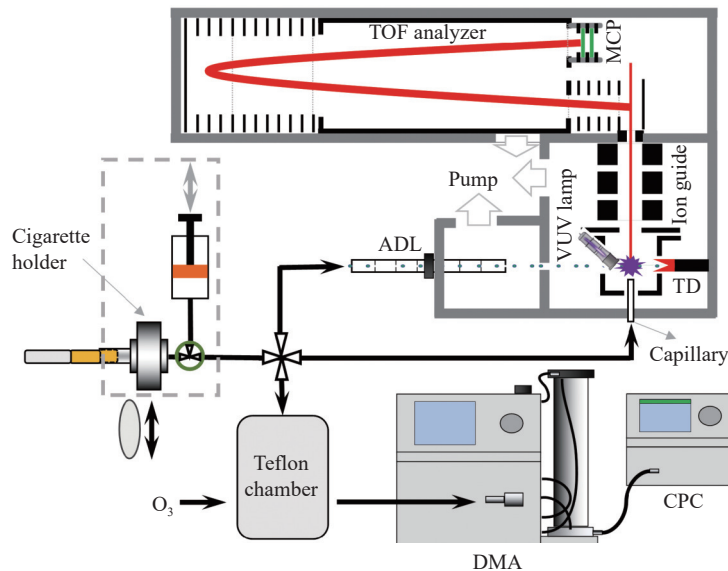


图1 实验装置示意图

Fig. 1 Schematic diagram of experimental apparatus

质谱的空气动力学透镜(ADL)进样系统进入。该 ADL 由一系列不同直径的薄板孔与垫环组成, 临界入口直径  $70\text{ }\mu\text{m}$ , 进样流量  $85\text{ cm}^3/\text{min}$ , 对于空气动力学直径约  $30\sim670\text{ nm}$  的颗粒物具有高效且一致的传输性, 基本覆盖了本实验 3 种烟气气溶胶的粒径范围。

经由毛细管进样的气相成分直接进入光电离室电离, 而通过 ADL 聚焦后的粒子束则需经过多级差分系统抽除气体, 仅颗粒物到达光电离室, 并在多孔钨制成的热脱附装置( $200\text{ }^\circ\text{C}$ )表面气化为气相分子, 随后被光电离。该质谱仪采用商用的氪放电灯( $h\nu = 10.0, 10.6\text{ eV}$ )作为光电离源对有机化合物进行软电离, 真空紫外光电离得到的样品离子由离子导入器(ion guide)垂直地引入到光电离质谱仪的 TOF 室中, 并直接到达质量分析器(TOF analyzer)的脉冲引出区域, 随后通过该反射式飞行时间质量分析器的双电场加速、双电场反射聚焦设计对样品离子进行分析。最后, 所有离子信号均由微通道板(MCP)进行检测, 并在经过前置放大器放大后由 P7888 采集卡(FAST ComTec, Germany)采集, 得到最终的光电离质谱信号。该光电离质谱的检测范围为  $1\sim350\text{ u}$ , 质量分辨率约  $2\,100$ (FWHM, full width at half maximum)。

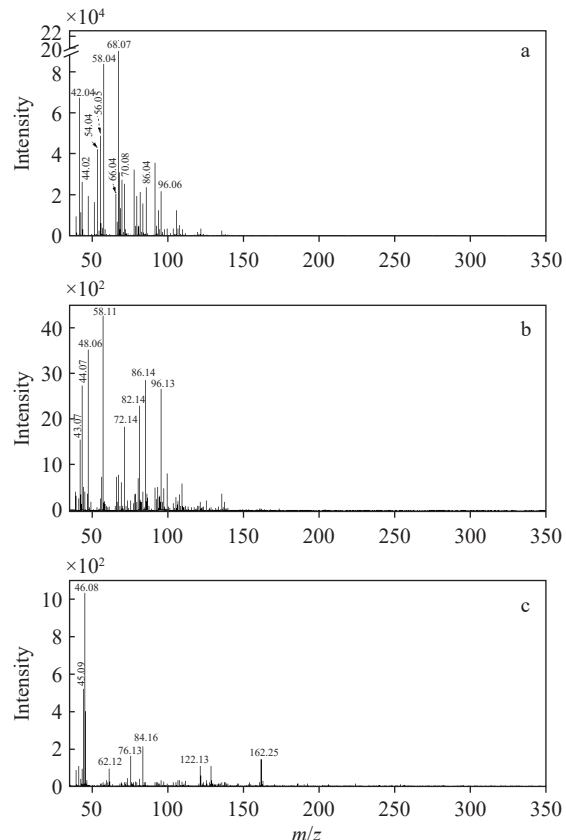
实验中使用的臭氧气体由小型臭氧发生器(Model 610, Jelight Company, Inc.)产生, 样品烟气气溶胶由吸烟机采集, 并控制所有实验组样品的气溶胶含量均为  $55\text{ cm}^3$ 。将  $55\text{ cm}^3$  烟气气溶胶充入预先用零空气填充了 98% 体积的 Teflon 反应袋( $150\text{ L}$ )中, 随后再向反应腔中充入一定量的臭氧进行老化反应模拟。使用扫描电迁移率粒径谱仪(SMPS, 美国 TSI 公司)实时监测烟气老化过程中的粒径分布及粒子数浓度变化, 该系统主要由差分迁移率分析仪(DMA, 3081)和凝聚核粒子计数器(CPC, 3776)组成。本实验设定扫谱范围为  $15\sim700\text{ nm}$ , 每张粒谱的扫描时间为  $3\text{ min}$ 。

## 2 结果与讨论

### 2.1 不同类型烟气气溶胶气相成分的光电离质谱表征

燃烧型卷烟、加热不燃烧型卷烟和电子烟烟气气溶胶中气相成分的光电离质谱图示于

图 2。在吸烟机抽吸量和光电离质谱进样流量保持相同的实验条件下, 一口( $55\text{ cm}^3$ )燃烧型卷烟烟气气溶胶中气相成分的光电离信号强度约为新型烟草制品的 100 倍。



注: a. 燃烧型卷烟; b. 加热不燃烧型卷烟; c. 电子烟

图 2 不同类型烟气气溶胶中气相成分的光电离质谱图

Fig. 2 Photoionization mass spectra of gas-phase composition in different smoke aerosols

由图 2a 可见, 燃烧型卷烟烟气气溶胶中的气相成分质谱峰集中分布于小质量区( $m/z < 140$ )。根据文献<sup>[30-32]</sup>报道对主要的检出峰进行指认, 发现大部分物质为不饱和化合物, 与 Zimmerman 等<sup>[22,24]</sup>的实验结果基本吻合。其中, 信号强度最高的 3 个峰为  $m/z$  68.07、58.04 和 42.04,  $m/z$  68.07 可指代  $\text{C}_4\text{H}_8\text{O}$ (呋喃)和  $\text{C}_5\text{H}_8$ (异戊二烯、环戊烯和 1,3-戊二烯),  $m/z$  58.04 可归属为  $\text{C}_3\text{H}_6\text{O}$ (丙酮、丙醛),  $m/z$  42.04 主要为  $\text{C}_3\text{H}_6$ (丙烯)。在其余强度较高的质谱峰中,  $m/z$  56.05 为丙烯醛和丁烯,  $m/z$  54.04 对应于 1,3-丁二烯和 1-丁炔,  $m/z$  70.08 主要来自戊烯和巴豆醛。此外, 气相部分还包括  $m/z$  44.02(乙醛)、66.04(1,3-环戊二烯)、86.04(2,3-丁二酮)、96.06(二甲基

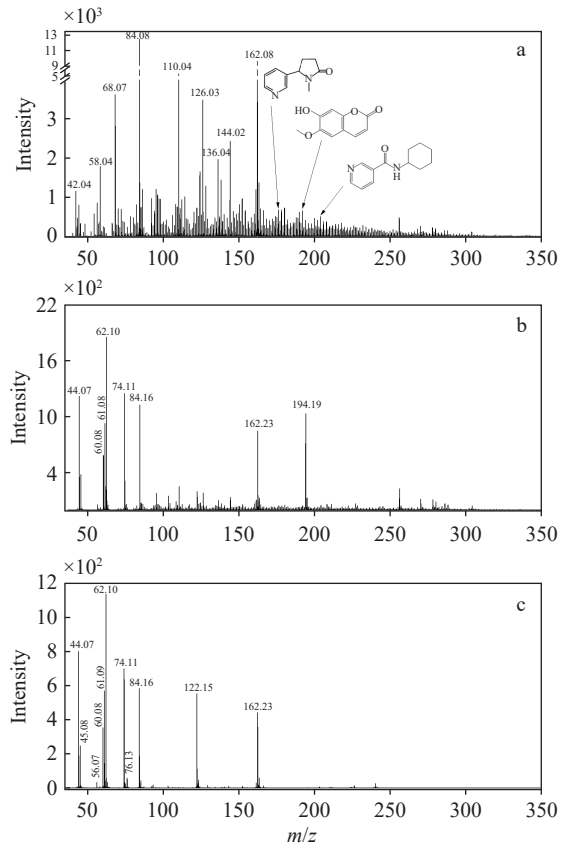
呋喃、糠醛)等。这些不饱和化合物中含有的不饱和化学键极易被室内氧化剂氧化而发生化学反应,促使烟气气溶胶在老化过程中形成超细颗粒物<sup>[33-34]</sup>。

由图2b可见,加热不燃烧型卷烟烟气气溶胶的气相光电离质谱分布与燃烧型卷烟相似,大部分质谱峰集中分布于小质量区( $m/z < 140.00$ ),但各物质的占比与燃烧型卷烟有较大差异。根据文献<sup>[5,29,35]</sup>报道,对主要的检出峰进行成分归属。其中,信号强度最高的3个峰为 $m/z$  44.07、48.06和58.11,可分别指代C<sub>2</sub>H<sub>4</sub>O(乙醛)、CH<sub>4</sub>S(甲硫醇)和C<sub>3</sub>H<sub>6</sub>O(丙醛、丙酮)。在稍宽的质量范围内,信号较强的质谱峰有 $m/z$  43.07、72.14、82.14、86.14和96.13,其中 $m/z$  43.07主要为碳氢化合物的碎片离子, $m/z$  72.14可能为丙烯酸、2-丁酮和异丁醛, $m/z$  82.14可能为2-甲基呋喃和2-环戊烯-1-酮, $m/z$  86.14可能为2,3-丁二酮、2-戊酮和正己烷, $m/z$  96.13可能为2,5-二甲基呋喃和糠醛。这些物质大多为不饱和化合物,在臭氧化过程中能够与O<sub>3</sub>反应,并导致超细颗粒物的生成。但由于其浓度远低于燃烧型卷烟,其在室内老化过程中的粒径分布可能与燃烧型卷烟存在差异。

与以上2种卷烟烟气复杂的气相成分分布不同,电子烟烟气气溶胶的气相光电离质谱较简单,且检出信号强度较低,示于图2c。结合文献<sup>[36-37]</sup>报道,对其中主要的光电离质谱峰进行成分归属,信号强度最高的质谱峰 $m/z$  46.08可归属为乙醇, $m/z$  45.09为气相的二甲胺、乙胺, $m/z$  122.13主要来源于苯甲酸。另外, $m/z$  62.12主要来自甘油的光电离碎片离子(C<sub>2</sub>H<sub>6</sub>O<sub>2</sub>)<sup>[38]</sup>, $m/z$  76.13来自丙二醇。甘油和丙二醇是电子烟烟液中填充的主要雾化剂成分。此外, $m/z$  162.25和84.16分别为尼古丁及其碎片离子<sup>[29]</sup>。

## 2.2 不同类型烟气气溶胶颗粒相成分的光电离质谱表征

不同类型烟气气溶胶颗粒相成分的光电离质谱图示于图3。相比于气相成分,颗粒相成分更为复杂。不同类型烟草制品产生的颗粒物成分分布完全不同,其中燃烧型卷烟颗粒相中的物质种类更丰富。在相同的实验条件下,一口(55 cm<sup>3</sup>)燃烧型卷烟烟气气溶胶中颗粒物的光电离信号强度约为新型烟草制品的10倍。



注: a. 燃烧型卷烟; b. 加热不燃烧型卷烟; c. 电子烟

图3 不同类型烟气气溶胶中颗粒相成分的  
光电离质谱图

Fig. 3 Photoionization mass spectra of particulate-phase composition in different smoke aerosols

如图3a所示,燃烧型卷烟烟气气溶胶的颗粒相组分非常复杂,几乎覆盖了质谱仪的整个扫描范围。强度最高的2个质谱峰为 $m/z$  162.08和84.08,分别对应尼古丁及其碎片离子<sup>[29]</sup>。结合文献<sup>[22,31,39]</sup>报道,对其余信号强度较高的质谱峰进行成分归属, $m/z$  110.04可指代C<sub>6</sub>H<sub>6</sub>O<sub>2</sub>(苯二酚、2-乙酰呋喃), $m/z$  126.03为C<sub>6</sub>H<sub>6</sub>O<sub>3</sub>(5-羟甲基糠醛), $m/z$  136.04主要为C<sub>10</sub>H<sub>16</sub>(柠檬烯), $m/z$  144.02对应C<sub>5</sub>H<sub>8</sub>O<sub>2</sub>(吡喃酮)和C<sub>6</sub>H<sub>8</sub>O<sub>4</sub>(1,4:3,6-二氢- $\alpha$ -d-吡喃葡萄糖)。以上化合物均含有不饱和化学键,容易在臭氧化过程中发生反应,促使超细颗粒物的形成。

加热不燃烧型卷烟烟气气溶胶中颗粒相的光电离质谱分布与燃烧型卷烟有明显差异,示于图3b。加热不燃烧型卷烟的颗粒相成分中含有大量甘油,其信号强度超过尼古丁,而在燃烧型

卷烟的颗粒相成分中却含量甚微。甘油的电离能为 9.4 eV, 在本实验的光电离源( $h\nu > 10$  eV)下, 甘油分子( $C_3H_8O_3$ ,  $m/z$  92)会解离为  $C_3H_6O_2^+$  ( $m/z$  74.11)、 $C_2H_6O_2^+$  ( $m/z$  62.10)、 $C_2H_5O_2^+$  ( $m/z$  61.08)、 $C_2H_4O_2^+$  ( $m/z$  60.08)和  $C_2H_4O^+$  ( $m/z$  44.07)等碎片离子<sup>[38]</sup>, 这些特征峰均在加热不燃烧型卷烟颗粒相的光电离质谱中得到确认, 且强度较高。此外, 在加热不燃烧型卷烟的颗粒相成分中具有较高占比的是尼古丁( $m/z$  84.16、162.23)和茄酮( $m/z$  194.19)<sup>[35]</sup>, 信号强度仅次于甘油。

相比于前 2 种卷烟烟气气溶胶, 电子烟烟气气溶胶的颗粒相成分更简单, 示于图 3c。电子烟的颗粒相成分中含有大量甘油,  $m/z$  44.07、

60.08、61.09、62.10 和 74.11 均来自甘油碎片离子的贡献;  $m/z$  84.16、162.23 可指代尼古丁;  $m/z$  122.15 主要来源于苯甲酸。此外,  $m/z$  45.08 可指代为乙胺;  $m/z$  56.07 为丙烯醛;  $m/z$  76.13 可归属为丙二醇, 是电子烟烟液中常见的雾化剂。

### 2.3 不同类型烟气气溶胶的室内老化模拟

在正常室内环境中, 臭氧浓度分布范围为小于  $10 \mu\text{g}/\text{m}^3$ ~大于  $100 \mu\text{g}/\text{m}^3$ <sup>[40]</sup>, 而在存在空气净化器、激光打印机和复印机等设备的环境中,  $O_3$  浓度可能会升高<sup>[41-42]</sup>。因此, 本研究控制臭氧浓度为 0、40、200  $\mu\text{g}/\text{m}^3$ , 分别模拟烟气气溶胶在无臭氧、低浓度臭氧和高浓度臭氧室内老化环境中的粒径分布, 结果示于图 4。

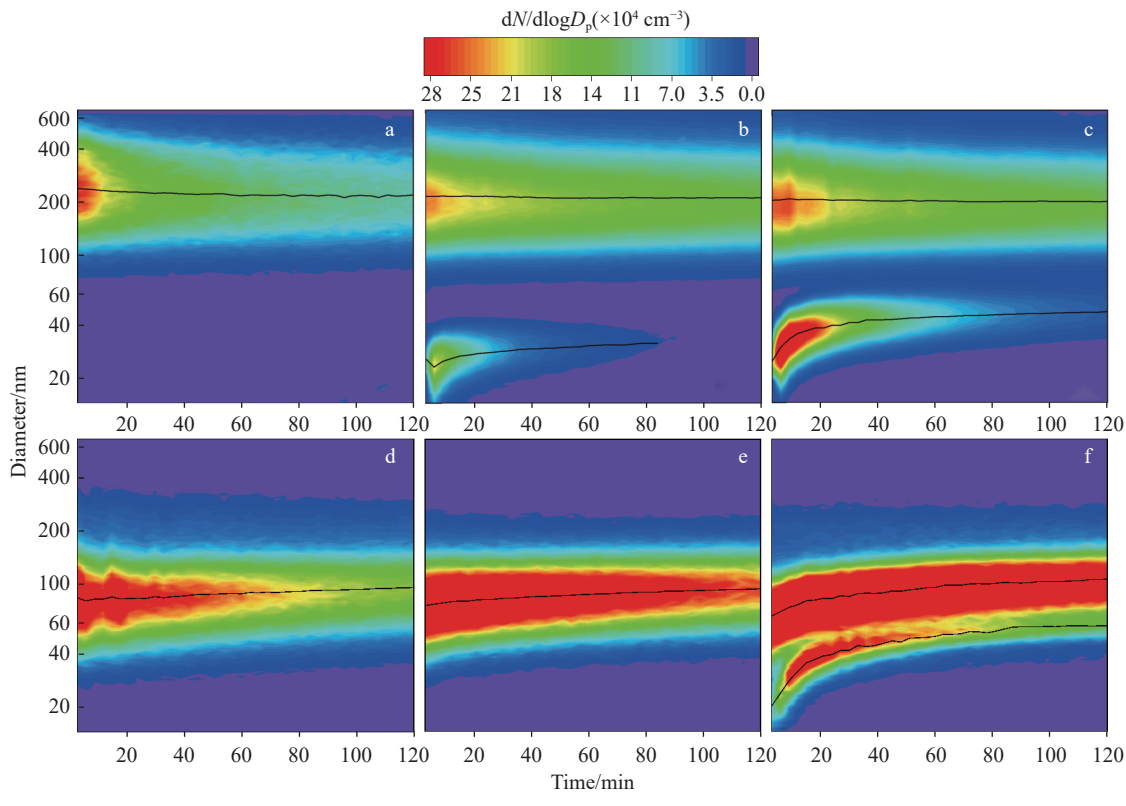


图 4 燃烧型(a, b, c)和加热不燃烧型(d, e, f)卷烟烟气气溶胶  
在室内环境不同臭氧浓度下的粒径分布

Fig. 4 Particle size distributions of combustion cigarette (a, b, c) and heat-not-burn (d, e, f) cigarette smoke in indoor environments with different concentrations of  $O_3$

当室内环境不存在  $O_3$  时, 传统燃烧型卷烟烟气气溶胶在 120 min 内的粒径整体呈单峰分布模式, 其初始几何平均直径约为 240 nm, 整体的粒径覆盖区间为 80~600 nm, 这与文献<sup>[24]</sup>报道一致, 示于图 4a; 当  $O_3$  浓度为 40  $\mu\text{g}/\text{m}^3$  时, 燃烧型

卷烟烟气气溶胶会与  $O_3$  反应, 形成的低挥发性物质作为新粒子的核产生初始几何平均直径约为 26 nm 的超细颗粒物, 气溶胶整体的粒径呈双峰分布模式, 示于图 4b。随着老化时间延长, 超细颗粒物的粒径不断增大, 这是由超细颗粒物自

身生长导致的,示于图4c。当反应进行到一定程度时,不再生成新的超细颗粒物,但仍存在反应腔内的壁损耗,导致粒子数浓度减小。

加热不燃烧型卷烟烟气气溶胶在无臭氧和低浓度臭氧环境中的粒径皆呈单峰分布模式,其初始几何平均直径约为80 nm,整体粒径覆盖区间为30~400 nm,示于图4d、4e。在200  $\mu\text{g}/\text{m}^3$  O<sub>3</sub>环境中,粒谱观测结果呈双峰分布,新生成的超细颗粒物的初始粒径约为20 nm,示于图4f。与燃烧型卷烟的老化情况相比,在样品抽吸量相同的情况下,加热不燃烧型卷烟烟气气溶胶形成超细颗粒物所需的O<sub>3</sub>浓度更高,表明其臭氧化形成超细颗粒物的过程更艰难。这是由于原始的加热不燃烧型卷烟烟气气溶胶的化学成分浓度远低于燃烧型卷烟,参与臭氧化反应的反应物很少,且其中含有大量几乎不存在于燃烧型卷烟中的甘油,由于甘油具有较强的粘黏性和包裹性,会通过包裹其他物质阻止老化进程。

在无臭氧环境中,电子烟产生的烟气气溶胶呈双峰向单峰过渡的分布模式,较大的粒径分布区间为100~600 nm,较小的为15~100 nm,示于图5a。这主要是由于电子烟颗粒物中含有大量的挥发性有机化合物,它们会逐渐由颗粒相挥发为气相,从而促使电子烟烟气气溶胶逐步过渡到以小颗粒为主的单峰分布模式,该结果与文献<sup>[43-45]</sup>报道一致。在40  $\mu\text{g}/\text{m}^3$  O<sub>3</sub>环境下,同样呈现由双峰向单峰过渡的分布模式,没有发现新的超细颗粒物生成;但在加入O<sub>3</sub>约30 min后,对于粒径小于100 nm的超细纳米范围,粒子数浓度略微上升,示于图5b。当将环境中的O<sub>3</sub>浓度提高至200  $\mu\text{g}/\text{m}^3$ 时,上升过程更加明显,示于图5c。与燃烧型卷烟的老化过程相比,电子烟生成超细颗粒物需要的时间更长,主要由于电子烟气溶胶中的化学成分浓度远小于燃烧型卷烟,导致参与臭氧化反应的反应物很少,且电子烟颗粒相中含有的大量甘油阻碍了老化进程。

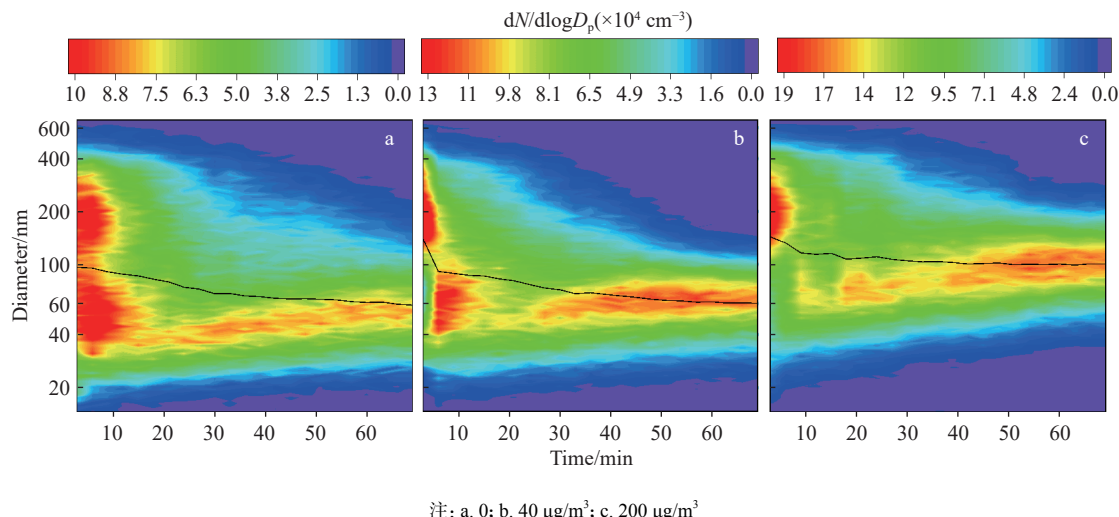


图5 电子烟烟气气溶胶在不同室内环境中的粒径分布

Fig. 5 Particle size distributions of e-cigarette smoke aerosols in indoor environment with different concentrations of O<sub>3</sub>

### 3 结论

本文基于自制的真空紫外光电离飞行时间质谱仪,原位在线检测了燃烧型卷烟、加热不燃烧型卷烟和电子烟烟气气溶胶的气相成分与颗粒相成分。采用Teflon反应腔模拟以上3种类型烟气气溶胶在不同臭氧浓度下的老化过程,并利用扫描电迁移率粒径谱仪表征它们在室内老化过程中的粒径分布。光电离质谱结果表明,3种烟气气溶胶的化学成分分布不同,燃烧型卷

烟的成分含量及物种丰度要远大于新型烟草制品,其气相和颗粒相信号强度分别约为新型烟草制品的100倍和10倍。此外,在烟气颗粒相的光电离质谱检测中发现,新型烟草制品中含有大量几乎不存在于燃烧型卷烟中的甘油,其信号强度甚至超过尼古丁。3种烟气气溶胶的室内老化过程不同,超细颗粒物的形成条件与前体物的含量和成分分布有关。具体表现为,室内浓度的O<sub>3</sub>(本实验中室内O<sub>3</sub>最低浓度为40  $\mu\text{g}/\text{m}^3$ )就

可以促使燃烧型卷烟烟气气溶胶生成新的几何平均直径约为26 nm的超细颗粒物,而新型烟草制品由于整体的化学成分浓度远小于燃烧型卷烟,且颗粒相中含有的大量甘油阻止了其老化进程,因而只有在更高浓度的O<sub>3</sub>或更长的老化时间下才能够形成超细颗粒物。

### 参考文献:

- [1] SOLEIMANI F, DOBARADARAN S, DE-LA-TORRE G E, SCHMIDT T C, SAEEDI R. Content of toxic components of cigarette, cigarette smoke vs cigarette butts: a comprehensive systematic review[J]. *Science of the Total Environment*, 2022, 813: 152 667.
- [2] HABRE R, DORMAN D C, ABBATT J, BAHNFLETH W P, CARTER E, FARMER D, GAWNE-MITTELSTAEDT G, GOLDSTEIN A H, GRASSIAN V H, MORRISON G, PECCIA J, POPPENDIECK D, PRATHER K A, SHIRAIWA M, STAPLETON H M, WILLIAMS M, HARRIES M E. Why indoor chemistry matters: a national academies consensus report[J]. *Environmental Science & Technology*, 2022, 56(15): 10 560-10 563.
- [3] FAGAN P, EISSENBERG T, JONES D M, COHEN J E, NEZ HENDERSON P, CLANTON M S. The first 10 years: reflecting on opportunities and challenges of the tobacco products scientific advisory committee of the United States food and drug administration[J]. *The Journal of Legal Medicine*, 2020, 40(3/4): 293-320.
- [4] SCHALLER J P, KELLER D, POGET L, PRATTE P, KAELIN E, McHUGH D, CUDAZZO G, SMART D, TRICKER A R, GAUTIER L, YERLY M, REIS PIRES R, Le BOUHELLEC S, GHOSH D, HOFER I, GARCIA E, VANSCHEEUWIJCK P, MAEDER S. Evaluation of the tobacco heating system 2.2. Part 2: chemical composition, genotoxicity, cytotoxicity, and physical properties of the aerosol[J]. *Regulatory Toxicology and Pharmacology*, 2016, 81: S27-S47.
- [5] FORSTER M, FIEBELKORN S, YURTERI C, MARINER D, LIU C, WRIGHT C, McADAM K, MURPHY J, PROCTOR C. Assessment of novel tobacco heating product THP1.0. Part 3: comprehensive chemical characterisation of harmful and potentially harmful aerosol emissions[J]. *Regulatory Toxicology and Pharmacology*, 2018, 93: 14-33.
- [6] DAVIS B, WILLIAMS M, TALBOT P. iQOS: evidence of pyrolysis and release of a toxicant from plastic[J]. *Tobacco Control*, 2019, 28(1): 34-41.
- [7] LI X, LUO Y, JIANG X, ZHANG H, ZHU F, HU S, HOU H, HU Q, PANG Y. Chemical analysis and simulated pyrolysis of tobacco heating system 2.2 compared to conventional cigarettes[J]. *Nicotine & Tobacco Research*, 2019, 21(1): 111-118.
- [8] RAWLINSON C, MARTIN S, FROSINA J, WRIGHT C. Chemical characterisation of aerosols emitted by electronic cigarettes using thermal desorption-gas chromatography-time of flight mass spectrometry[J]. *Journal of Chromatography A*, 2017, 1497: 144-154.
- [9] 陆怡峰, 李永霞, 张珲姿, 刘鸿, 姚鹤鸣, 郑赛晶, 陈勇. 电感耦合等离子体质谱法同时测定电子烟气溶胶中7种重金属元素[J]. *分析测试学报*, 2020, 39(6): 729-735. LU Yifeng, LI Yongxia, ZHANG Huizi, LIU Hong, YAO Heming, ZHENG Saijing, CHEN Yong. Simultaneous determination of heavy metal elements in e-cigarette aerosols by inductively coupled plasma mass spectrometry[J]. *Journal of Instrumental Analysis*, 2020, 39(6): 729-735(in Chinese).
- [10] PETRICK L M, SLEIMAN M, DUBOWSKI Y, GUNDEL L A, DESTAILLATS H. Tobacco smoke aging in the presence of ozone: a room-sized chamber study[J]. *Atmospheric Environment*, 2011, 45(28): 4 959-4 965.
- [11] BORDUAS N, MURPHY J G, WANG C, Da SILVA G, ABBATT J P D. Gas phase oxidation of nicotine by OH radicals: kinetics, mechanisms, and formation of HNCO[J]. *Environmental Science & Technology Letters*, 2016, 3(9): 327-331.
- [12] PETRICK L M, SVODOVSKY A, DUBOWSKI Y. Thirdhand smoke: heterogeneous oxidation of nicotine and secondary aerosol formation in the indoor environment[J]. *Environmental Science & Technology*, 2011, 45(1): 328-333.
- [13] SLEIMAN M, DESTAILLATS H, SMITH J D, LIU C L, AHMED M, WILSON K R, GUNDEL L A. Secondary organic aerosol formation from ozone-initiated reactions with nicotine and secondhand tobacco smoke[J]. *Atmospheric Environment*, 2010, 44(34): 4 191-4 198.
- [14] SLEIMAN M, GUNDEL L A, PANKOW J F, JACOB P, SINGER B C, DESTAILLATS H. Formation of carcinogens indoors by surface-mediated reactions of nicotine with nitrous acid, leading to potential thirdhand smoke hazards[J]. *Proceedings of the National Academy of Sciences of the United States of America*, 2010, 107(15): 6

- 576-6 581.
- [15] WANG C, COLLINS D B, HEMS R F, BORDUAS N, ANTIÑOLO M, ABBATT J P D. Exploring conditions for ultrafine particle formation from oxidation of cigarette smoke in indoor environments[J]. Environmental Science & Technology, 2018, 52(8): 4 623-4 631.
- [16] LIM D H, KIM Y H, SON Y S, JO S H, KIM K H. A simple sampling method for quantification of hazardous volatile organic compounds in mainstream cigarette smoke: method development and prestudy validation[J]. Microchemical Journal, 2022, 180: 107 602.
- [17] SAVAREEAR B, ESCOBAR-ARNANZ J, BROKL M, SAXTON M J, WRIGHT C, LIU C, FOCANT J F. Non-targeted analysis of the particulate phase of heated tobacco product aerosol and cigarette mainstream tobacco smoke by thermal desorption comprehensive two-dimensional gas chromatography with dual flame ionisation and mass spectrometric detection[J]. Journal of Chromatography A, 2019, 1 603: 327-337.
- [18] 贾春晓, 黄备备, 杨鹏飞, 陈芝飞, 席高磊, 毛多斌. 同位素稀释-气相色谱-质谱联用法分析烟气中性香味成分[J]. 质谱学报, 2019, 40(6): 565-574.  
JIA Chunxiao, HUANG Beibei, YANG Pengfei, CHEN Zhifei, XI Gaolei, MAO Duobin. Neutral aromatic components from cigarette smoke by isotope dilution-GC/MS[J]. *Journal of Chinese Mass Spectrometry Society*, 2019, 40(6): 565-574(in Chinese).
- [19] THIELEN A, KLUS H, MÜLLER L. Tobacco smoke: unraveling a controversial subject[J]. Experimental and Toxicologic Pathology, 2008, 60(2/3): 141-156.
- [20] LIU B, LI Y M, WU S B, LI Y H, DENG S S, XIA Z L. Pyrolysis characteristic of tobacco stem studied by py-GC/MS, TG-FTIR, and TG-MS[J]. BioResources, 2012, 8(1): 220-230.
- [21] SHI Q, NELSON D D, McMANUS J B, ZAHNISER M S, PARRISH M E, BAREN R E, SHAFER K H, HARDWARD C N. Quantum cascade infrared laser spectroscopy for real-time cigarette smoke analysis[J]. Analytical Chemistry, 2003, 75(19): 5 180-5 190.
- [22] MITSCHKE S, ADAM T, STREIBEL T, BAKER R R, ZIMMERMANN R. Application of time-of-flight mass spectrometry with laser-based photoionization methods for time-resolved on-line analysis of mainstream cigarette smoke[J]. Analytical Chemistry, 2005, 77(8): 2 288-2 296.
- [23] ADAM T, MITSCHKE S, STREIBEL T, BAKER R R, ZIMMERMANN R. Puff-by-puff resolved characterisa-
- tion of cigarette mainstream smoke by single photon ionisation (SPI)-time-of-flight mass spectrometry (TOF MS): comparison of the 2R4F research cigarette and pure Burley, Virginia, Oriental and Maryland tobacco cigarettes[J]. *Analytica Chimica Acta*, 2006, 572(2): 219-229.
- [24] ADAM T, McAUGHEY J, MCGRATH C, MOCKER C, ZIMMERMANN R. Simultaneous on-line size and chemical analysis of gas phase and particulate phase of cigarette mainstream smoke[J]. Analytical and Bioanalytical Chemistry, 2009, 394(4): 1 193-1 203.
- [25] BARSANTI K C, LUO W, ISABELLE L M, PANKOW J F, PEYTON D H. Tobacco smoke particulate matter chemistry by NMR[J]. *Magnetic Resonance in Chemistry*, 2007, 45(2): 167-170.
- [26] YADAV R, SAOUD K, RASOULI F, HAJALIGOL M, FENNER R. Study of cigarette smoke aerosol using time of flight mass spectrometry[J]. *Journal of Analytical and Applied Pyrolysis*, 2004, 72(1): 17-25.
- [27] WANG X, JIANG Q, LI H, CHEN D. Rapid determination of chemical composition in the particulate matter of cigarette mainstream smoke[J]. Talanta, 2020, 217: 121 060.
- [28] PHARES D J, COLLIER S, ZHENG Z, JUNG H S. *In-situ* analysis of the gas- and particle-phase in cigarette smoke by chemical ionization TOF-MS[J]. *Journal of Aerosol Science*, 2017, 106: 132-141.
- [29] WEN Z, GU X, TANG X, LI X, PANG Y, HU Q, WANG J, ZHANG L, LIU Y, ZHANG W. Time-resolved online analysis of the gas- and particulate-phase of cigarette smoke generated by a heated tobacco product using vacuum ultraviolet photoionization mass spectrometry[J]. Talanta, 2022, 238: 123 062.
- [30] PAN Y, HU Y, WANG J, YE L, LIU C, ZHU Z. Online characterization of isomeric/isobaric components in the gas phase of mainstream cigarette smoke by tunable synchrotron radiation vacuum ultraviolet photoionization time-of-flight mass spectrometry and photoionization efficiency curve simulation[J]. Analytical Chemistry, 2013, 85(24): 11 993-12 001.
- [31] 赵锋, 温作赢, 顾学军, 王健, 唐小锋, 张为俊. 真空紫外光电离质谱在线检测卷烟主流烟气气溶胶中气体和颗粒物的化学成分[J]. 质谱学报, 2023, 44(6): 770-779.  
ZHAO Feng, WEN Zuoying, GU Xuejun, WANG Jian, TANG Xiaofeng, ZHANG Weijun. On-line analysis of chemical components of gas-phase and particulate-phase in cigarette mainstream smoke by vacuum ultraviolet

- photoionization mass spectrometry[J]. *Journal of Chinese Mass Spectrometry Society*, 2023, 44(6): 770-779 (in Chinese).
- [32] CHARLES S M, BATTERMAN S A, JIA C. Composition and emissions of VOCs in main- and side-stream smoke of research cigarettes[J]. *Atmospheric Environment*, 2007, 41(26): 5 371-5 384.
- [33] DESTAILLATS H, LUNDEN M M, SINGER B C, COLEMAN B K, HODGSON A T, WESCHLER C J, NAZAROFF W W. Indoor secondary pollutants from household product emissions in the presence of ozone: a bench-scale chamber study[J]. *Environmental Science & Technology*, 2006, 40(14): 4 421-4 428.
- [34] FAN Z, WESCHLER C J, HAN I K, ZHANG J. Co-formation of hydroperoxides and ultra-fine particles during the reactions of ozone with a complex VOC mixture under simulated indoor conditions[J]. *Atmospheric Environment*, 2005, 39(28): 5 171-5 182.
- [35] BENTLEY M C, ALMSTETTER M, ARNDT D, KNORR A, MARTIN E, POSPISIL P, MAEDER S. Comprehensive chemical characterization of the aerosol generated by a heated tobacco product by untargeted screening[J]. *Analytical and Bioanalytical Chemistry*, 2020, 412(11): 2 675-2 685.
- [36] NAEEM M N M, ZAIN S M S M, NG C, NOH M F M. Chemical constituents in e-cigarette liquids and aerosols[J]. *Journal of Environmental Protection*, 2020, 11(9): 664-681.
- [37] CUNNINGHAM A, McADAM K, THISSEN J, DIGARD H. The evolving e-cigarette: comparative chemical analyses of e-cigarette vapor and cigarette smoke[J]. *Frontiers in Toxicology*, 2020, 2: 586 674.
- [38] BELL F, RUAN Q N, GOLAN A, HORN P R, AHMED M, LEONE S R, HEAD-GORDON M. Dissociative photoionization of glycerol and its dimer occurs predominantly via a ternary hydrogen-bridged ion-molecule complex[J]. *Journal of the American Chemical Society*, 2013, 135(38): 14 229-14 239.
- [39] ZHAO F, WEN Z, GU X, ZHANG W, TANG X. Operando gas- and particle-phase measurements of combustion cigarette smoke aerosols by vacuum ultraviolet photoionization mass spectrometry[J]. *Journal of Aerosol Science*, 2024, 178: 106 358.
- [40] FADEYI M O. Ozone in indoor environments: research progress in the past 15 years[J]. *Sustainable Cities and Society*, 2015, 18: 78-94.
- [41] HUBBARD H F, COLEMAN B K, SARWAR G, CORSI R L. Effects of an ozone-generating air purifier on indoor secondary particles in three residential dwellings[J]. *Indoor Air*, 2005, 15(6): 432-444.
- [42] DESTAILLATS H, MADDALENA R L, SINGER B C, HODGSON A T, McKONE T E. Indoor pollutants emitted by office equipment: a review of reported data and information needs[J]. *Atmospheric Environment*, 2008, 42(7): 1 371-1 388.
- [43] FUOCO F C, BUONANNO G, STABILE L, VIGO P. Influential parameters on particle concentration and size distribution in the mainstream of e-cigarettes[J]. *Environmental Pollution*, 2014, 184: 523-529.
- [44] MIKHEEV V B, IVANOV A, LUCAS E A, SOUTH P L, COLIJN H O, CLARK P I. Aerosol size distribution measurement of electronic cigarette emissions using combined differential mobility and inertial impaction methods: Smoking machine and puff topography influence[J]. *Aerosol Science and Technology*, 2018, 52(11): 1 233-1 248.
- [45] PAPAEFSTATHIOS E, BEZANTAKOS S, STYLIANOU M, BISKOS G, AGAPIOU A. Comparison of particle size distributions and volatile organic compounds exhaled by e-cigarette and cigarette users[J]. *Journal of Aerosol Science*, 2020, 141: 105 487.

(收稿日期: 2024-03-18; 修回日期: 2024-04-18)